World Journal of Urology (2019) 37:1339–1346
https://doi.org/10.1007/s00345-018-2520-3

ORIGINAL ARTICLE

Can contrast-enhanced ultrasound and acoustic radiation force impulse imaging characterize CT-indeterminate renal masses? A prospective evaluation with histological confirmation

Wolfgang M. Thaiss[1] · Jens Bedke[2] · Stephan Kruck[2] · Daniel Spira[3] · Arnulf Stenzl[2] · Konstantin Nikolaou[1] · Marius Horger[1] · Sascha Kaufmann[1]

Received: 5 June 2018 / Accepted: 6 October 2018 / Published online: 15 October 2018

Abstract

Purpose To prospectively characterize computed tomography (CT)-indeterminate renal masses (CTIRM) using acoustic radiation force impulse (ARFI) elastography and contrast-enhanced ultrasound (CEUS) and to correlate quantitative imaging findings with histopathology or interim follow-up (FU).

Methods 123 patients with CTIRM (longest diameter < 4 cm) underwent ARFI and CEUS with CT image fusion (IF). Exclusion criteria included all contraindications for CEUS and IF. Shear wave velocity (SWV), shear wave ratio (SWR), peak intensity (PE), time to peak (TTP) and wash-in rate (Wi) were quantified. In case of a cystic lesion classified as ≤ Bosniak 2F, follow-up imaging was performed.

Results 77 out of 123 patients underwent surgical resection of a lesion due to suspect imaging findings, whereas 46 patients underwent FU, which did not show upgrading in Bosniak category. Histopathology revealed 58 renal cell carcinomas [five chromophobe (chRCC), 18 papillary (pRCC) and 35 clear cell (ccRCC)], ten oncocytomas and nine non-malignant renal lesions (one minimal fat AML, three focal nephritis and five infected cysts). SWV and SWR differed significantly between ccRCC, pRCC, chRCC ($p = 0.0024$, $F = 13.94$) and in SWR also for oncocytoma ($p < 0.0001$, $F = 14.35$). In CEUS, oncocytoma and ccRCC showed significant higher PE values ($p < 0.0001$, $F = 77.31$) as well as higher Wi and lower TTP compared to all other solid lesions.

Conclusions Quantitative CEUS and ARFI imaging can provide relevant information to further characterize CT-indeterminate renal masses to guide urological decision making and offer the possibility of differentiation between ccRCC from less malignant RCC subtypes and from oncocytoma.

Keywords CEUS · Ultrasound · Indeterminate renal masses · ARFI

Abbreviations

ARFI	Acoustic radiation force impulse
CEUS	Contrast-enhanced ultrasound
CT	Computed tomography
CECT	Contrast-enhanced computed tomography
DCE-MRI	Dynamic contrast-enhanced magnet resonance tomography
PE	Peak enhancement
TTP	Time to peak
CTIRM	CT-indeterminate renal masses
SWV	Shear wave velocity
SWR	SWV ratio
US	Ultrasound
WiAUC	Area under the curve (wash-in)

Introduction

Growing examination numbers in abdominal imaging lead to an increased detection of indeterminate renal masses in asymptomatic individuals [1]. Renal masses are often incidentally detected in contrast-enhanced computed tomography (CECT) performed for other reasons. Differentiation between benign and malignant lesions is challenging in

Electronic supplementary material The online version of this article (https://doi.org/10.1007/s00345-018-2520-3) contains supplementary material, which is available to authorized users.

✉ Jens Bedke
jens.bedke@med.uni-tuebingen.de

Extended author information available on the last page of the article

urological practice but determines the subsequent urological treatment or follow-up. An indeterminate renal mass is defined as "a lesion that cannot be diagnosed confidently as benign or malignant when discovered" [1]. Most of the routinely performed CECTs use only one contrast phase of the kidneys, thus enhancement patterns are not available to differentiate innate hyperdense lesions (e.g., hyperdense cysts) from solid lesions. In solid renal masses, surgical resection is usually performed because reliable identification of benign tumors like oncocytoma by imaging is considered challenging [2]. If lesions are categorized as indeterminate, work-up with multiphase CECT is still the gold standard for characterization of renal tumors and complicated cysts [3]. Beside multiphase CECT, dynamic contrast-enhanced magnetic resonance imaging (DCE-MRI) or contrast-enhanced ultrasound (CEUS) can characterize renal lesions. The potential nephrotoxic effect of iodinated contrast media and gadolinium-based MR contrast media, higher potential for allergic reactions to these contrast agents, higher costs and restricted availability of MRI limit their use in clinical routine.

Today, preoperative imaging of renal lesions is still far from ideal as 25–30% of resected lesions are benign or indolent and may not require surgery [4]. Besides differentiation of benign lesions from renal cell carcinoma (RCC), differentiation of RCC subtypes on imaging is difficult [5, 6]. However, preoperative imaging-based differentiation and further subtyping of RCCs has prognostic significance, as clear cell renal carcinoma (ccRCC) and other rare subtypes including collecting duct, papillary type 2, and medullary RCC are aggressive tumors, while papillary type 1 (pRCC), chromophobe (chRCC) and multilocular cystic lesions with unknown malignant potential seem to be more indolent [7–10].

Currently, research using different features of ultrasound technology for differentiating subtypes of RCC is growing. Multimodality fusion imaging systems have been developed recently for improvement of lesion detection and characterization. As malignant tissues are generally stiffer than benign, the evaluation of tissue elasticity might be useful for the characterization of renal masses [11]. Acoustic radiation force impulses (ARFI) can be used as an additional ultrasonographic technique in the differentiation of benign and malignant lesions since the diagnostic accuracy of B-mode ultrasound is low. CEUS is described as superior to CECT with respect to intralesional vascularity [12]. To date, no prospective study has reported imaging characterization of small incidentally detected CT-intermediate lesions by quantitative elastography using ARFI and quantitative CEUS after image fusion.

Hence, the purpose of this work was to prospectively evaluate quantitative imaging parameters derived from ARFI and CEUS for differentiating indeterminate renal masses detected on CT into benign and different subtypes of malignancy.

Materials and methods

Patient characteristics

This prospective study was approved by the institutional review board (361/2015BO2), and informed consent was obtained. Patients with an incidental finding of a CT-indeterminate renal mass smaller than 4 cm in diameter [13] were planned for routine B-mode ultrasound and offered B-mode ultrasound with image fusion (IF) and additional imaging with ARFI and CEUS. Bosniak classification was applied to cystic lesions in accordance with CT and B-mode ultrasound. In case of a cystic lesion ≤ Bosniak 2F, follow-up was performed. Patients were enrolled between July 2015 and May 2016. Exclusion criteria include all contraindications for CEUS with SonoVue® (Bracco, Italy) such as evidence of chronic kidney disease and additional contraindications of CT/US image fusion like cardiac pacemakers. The ultrasound examination was performed within 7 days (range 0–7) related to the baseline CT examination and in case of surgical resection within 10 days before surgery. The examination time per patient included IF, B-mode ultrasound, power Doppler ultrasound (PDUS), ARFI and CEUS. Details on the imaging performed are given in the Supplement Material.

Statistical analysis

Summary statistics of the measured shear wave velocity (SWV) and shear wave ratio (SWR) from ARFI as well as the perfusion parameters from CEUS are reported as mean and standard deviation. Groups were compared using one-way ANOVA. For all tests, p values smaller than 0.05 were considered significant. p values were adjusted for multiple testing. The calculations were performed using Prism 6 (GraphPad software, La Jolla, CA, USA).

Results

Between July 2015 and May 2016, 123 patients (male 77; mean age 64 years; range 32–79 years) were included with an incidental finding of a renal lesion that could not be diagnosed confidently as benign or malignant in primary contrast-enhanced CT, therefore defined as CTIRM in CECT. All patients underwent IF for lesion detection and characterization, B-mode ultrasound with PDUS, ARFI imaging and CEUS imaging. As described above, pure cystic lesions or

cystic lesions without a relevant solid component were not evaluated with ARFI.

No adverse reactions to contrast media administration were encountered. Mean lesion diameter was 2.1 cm (range 1.2–3.6 cm). Lesions showed a wide range of hyper-, hypo- or isoechogenicity compared with renal parenchyma, but echogenicity showed no correlation with histopathology except for cystic lesions, which showed the typical hypoechogenicity. PDUS showed vascular flow in 39/123 lesions (32%). Only patients with solid lesions (ccRCC, pRCC, chRCC, minimal fat angiomyolipoma or oncocytoma) showed vascular flow in PDUS, but PDUS shows no significant differences between these different tumor entities. Mean examination time per patient including IF, PDUS, ARFI and CEUS was 14 min. Altogether, 51 lesions (41%) were classified as cystic in categories according to the Bosniak classification system, and 72 lesions (59%) were classified as solid. Five of the cystic lesions had a complex cystic appearance and were rated as category III and underwent surgical resection. Histologically, all category III cysts showed no signs of malignancy but signs of chronic inflammation and fibrosis, and thus were classified as chronic-infected cysts. 58/72 solid lesions (81%) were histologically classified as renal cell carcinoma (ccRCC: $n=35$, pRCC type 1: $n=18$ and chRCC: $n=5$), whereas 10/72 lesions (14%) were classified as oncocytoma. 1/72 (1%) minimal fat angiomyolipoma and 3/72 (4%) chronic focal nephritis were defined (Fig. 1). The non-resected cystic lesions ($n=46$) included five lesions in category I, 30 in category II and 11 in category IIF according to the Bosniak classification. All cystic lesions were followed with ultrasound and/or MRI/CT for a minimum of 24 months and all lesions were stable in size and category.

Acoustic radiation force impulse (ARFI) imaging

The lesions were located in a mean depth of 5.7 cm (range 3.4–7.5 cm). No significant differences concerning lesion depth were observed between different tumor entities. Performing ARFI quantification, mean tissue shear velocities for renal lesions was 2.7 m/s (range 0.7–4.96 m/s). Renal parenchyma mean tissue shear velocity was 2.0 m/s (range 1.5–2.8 m/s). Mean SWV and SWR stratified by histology are summarized in the Supplement Material. ccRCC showed SWV of 3.4 ± 0.8 m/s that was significantly higher compared to pRCC (2.2 ± 1.0 m/s, $p < 0.001$) and chRCC (1.9 ± 0.5 m/s, $p = 0.0024$, $F = 13.94$). Significant higher ratios (SWR) between ROI_{lesion} and normal renal cortex ($ROI_{parenchyma}$) were present in ccRCC (1.8 ± 0.4

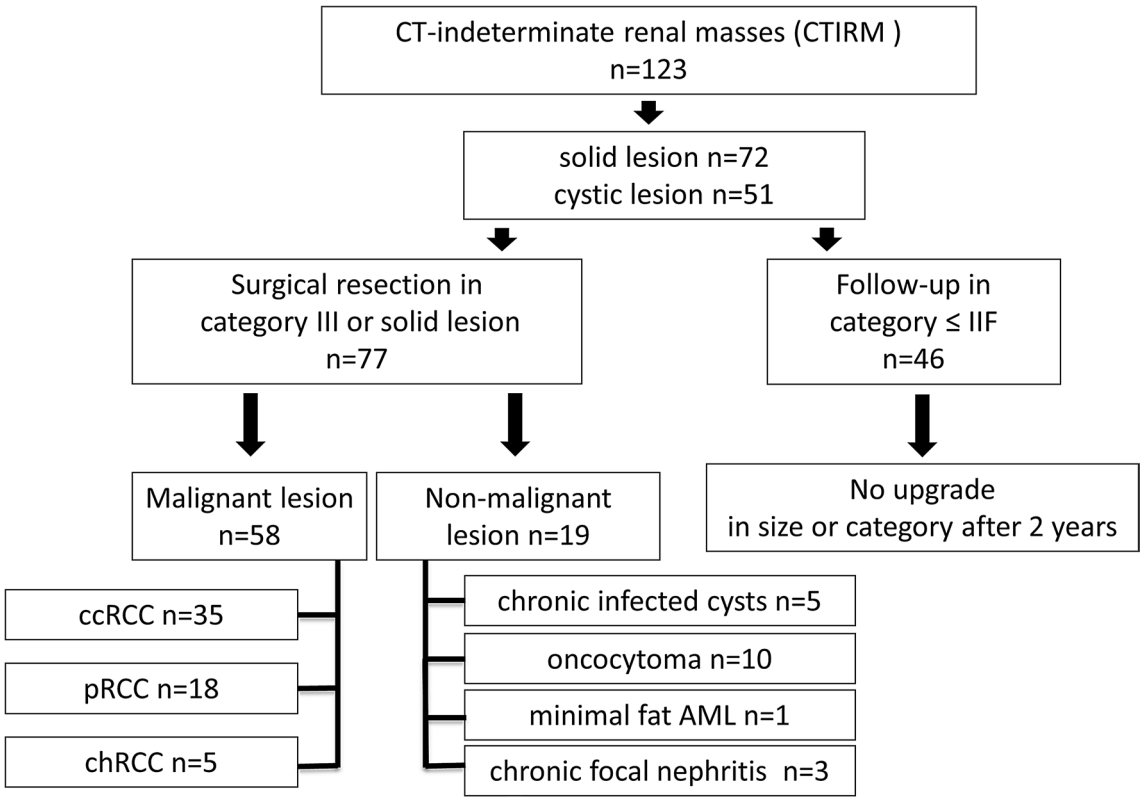

Fig. 1 Flow chart for included CT-intermediate renal lesions

compared to 1.1 ± 0.5 in pRCC, $p < 0.001$; 1.0 ± 0.1 in chRCC, $p = 0.02$; 1.6 ± 0.3 in oncocytoma, $p < 0.0001$, $F = 14.35$).

Contrast-enhanced ultrasound (CEUS)

Peak enhancement in ccRCC and oncocytoma showed higher values compared to all other entities (194.0 ± 43.8% for ccRCC and 135.9 ± 28.1% for oncocytoma; $p < 0.0001$, $F = 77.31$). Additionally, significant differences were present between ccRCC and oncocytoma ($p < 0.0001$, Fig. 2a and Table 1 in Supplement Material). TTP was close to each other, and we observed significant differences between oncocytoma (101.9 ± 11.8%) and ccRCC (87.4 ± 13.0%, $p = 0.01$, $F = 9.1$) and furthermore between ccRCC and the different renal cell carcinoma subtypes (pRCC 109.6 ± 8.8%, chRCC 106.9 ± 22.3%, $p < 0.0001$ and $p = 0.02$, respectively). Oncocytoma (126.2 ± 20.5%) and ccRCC (189.4 ± 56.8%) showed significantly higher values for wash-in compared to all other entities ($p = 0.009$, Fig. 2b). Significant differences between oncocytoma (101.9 ± 11.8%) and ccRCC were observed (87.4 ± 13.0%, $p = 0.01$, $F = 9.1$) as well as between ccRCC and the different renal cell carcinoma subtypes (pRCC 109.6 ± 8.8%, chRCC 106.9 ± 22.3%, $p < 0.0001$ and $p = 0.02$, respectively). The results of quantitative data analysis from CEUS are summarized in the Supplement Material. Patient examples for a malignant and a non-malignant lesion are given in Fig. 3.

Discussion

The increased number of incidental renal findings due to an overall increase in abdominal CT-imaging leads to detection of indeterminate renal masses (CTIRM). Multiphase CT with unenhanced and enhanced phases is still the gold standard for characterization of renal lesions, but the evaluation of enhancement can be difficult [14].

Therefore, the aim of this study was to use advanced quantitative ultrasound methods (ARFI and CEUS) to differentiate CTIRM. As described in other studies, effectiveness of CEUS can decrease if the lesion cannot be adequately identified by US. Therefore, quantitative imaging with ARFI and CEUS after US/CT image fusion was performed [15]. To our knowledge, this study is the largest series to examine both benign lesions including oncocytomas and different types of RCC with quantitative ARFI and CEUS after image fusion. All cystic lesions classified as Bosniak 2F and without histological confirmation were followed over a minimum of 24 months without upgrading according to the Bosniak classification.

ARFI elastography has been introduced in the last years, but only a few studies with small patient numbers systematically evaluated ARFI elastography in renal lesions [16]. The main limitation of ARFI imaging is the lack of quantification from pure cystic lesions or cystic lesions with thin septa without solid components. Thus, ARFI imaging can only be validly performed for solid or cystic lesions with a relevant solid component. We observed significant differences in SWV between histologically proven ccRCC

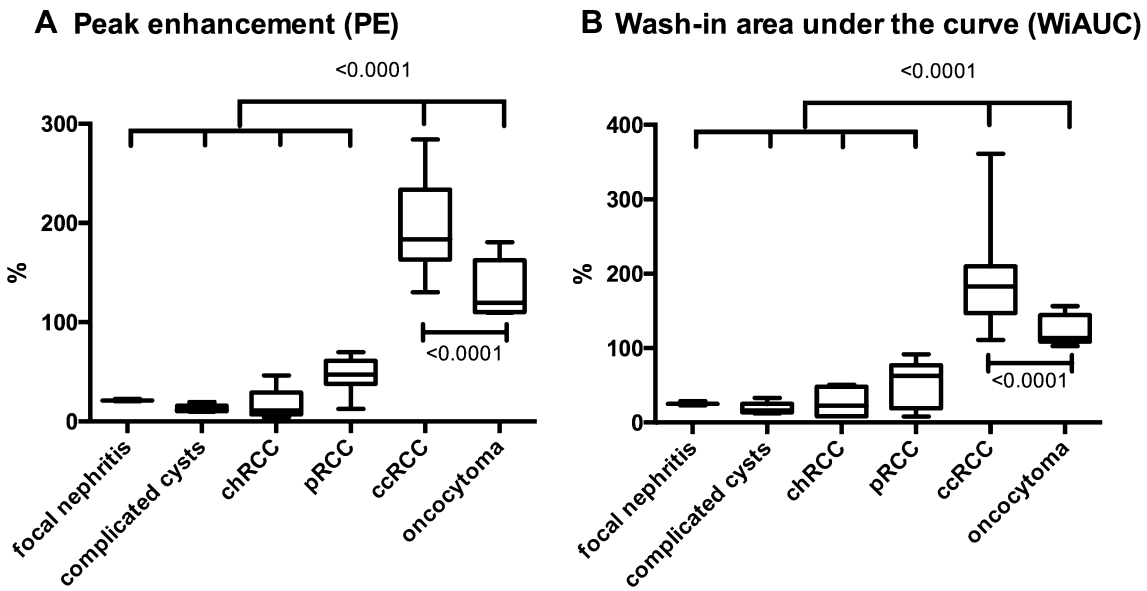

Fig. 2 Box plots for CEUS evaluation: peak enhancement (**a**) and wash-in area under the curve (**b**). *p* values from ANOVA are indicated for group comparisons

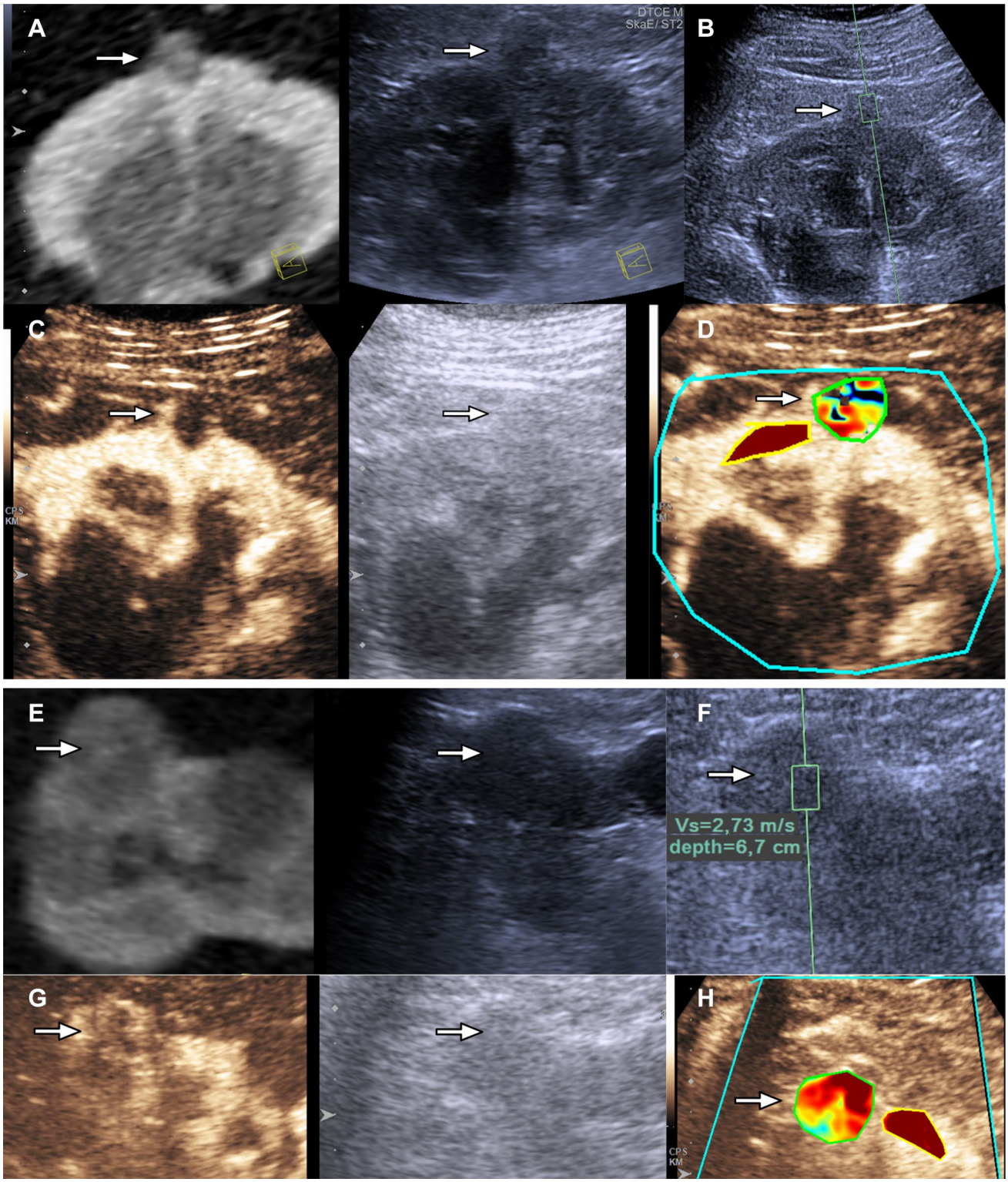

Fig. 3 53-year-old male patient with incidentally detected renal mass on CECT. Image fusion in side-by-side view shows a small lesion (**a**, arrow) of the left kidney (left, angulated CT image). The corresponding B-mode sonography (right) reveals a lesion with nearly no echogenicity and presence of distal acoustic enhancement. ARFI mode reveals an increased SWV of 3.82 m/s (**b**). CEUS (**c**, left) reveals a lesion with wall enhancement; histology showed a cystic lesion with chronic inflammation and fibrosis. Quantification of CEUS parameters (**d**). **e**–**h** Show a 71-year-old male patient with an incidentally detected renal mass on CECT. Image fusion shows a small lesion (**e**, arrow) of the left kidney (left, angulated CT image). The corresponding B-mode sonography (right) reveals a lesion with low echogenicity and the presence of distal acoustic enhancement. ARFI mode reveals an increased SWV of 2.73 m/s (**f**). CEUS (**g**, left) reveals a lesion with inhomogeneous enhancement; histology showed a pRCC. Quantification of CEUS parameters (**h**)

compared to pRCC and chRCC. The SWV of solid components of chronic-infected cysts were significantly lower compared to all other solid lesions. Significantly higher ratios between ROI_{lesion} and $ROI_{parenchyma}$ were present in ccRCC in comparison to other RCC subtypes or to oncocytoma. A study from Clevert et al. with 12 histological proven renal lesions, reported that elastography has the potential to differentiate between benign and malignant renal lesions [16]. Göya et al. reported that classical AML with macroscopic fat content shows relevant lower SWV value than RCC values ($p = 0.002$). However, other methods like B-mode ultrasound, CT and MRI detect macroscopic fat and AMLs with poor fat content were not included in this study [17]. Furthermore, they did not find significant differences between the RCC subgroups and further differentiation between infectious lesions and RCC with SWV values was not possible, which is in line with our findings. In comparison to their study, we could include a relevant number of oncocytomas, which represent the most frequent benign differential diagnosis to RCC. This entity could be separated from ccRCC with respect to their SWV values by AFRI.

CEUS allows the evaluation of macro- and especially microvascular enhancement with higher temporal and space-related resolution compared to CT and MRI and was shown to be more sensitive than CECT and MRI in detecting intralesional vascularity [18]. Our quantitative results showed that ccRCC and oncocytoma had higher values for PE compared to all other entities but also discernable from one another. With regard to wash-in, oncocytoma and ccRCC showed significantly higher values than other entities. We observed significant differences for TTP between oncocytoma and ccRCC and furthermore between ccRCC and pRCC, as well as chRCC.

Barr et al. analyzed the CEUS pattern of 596 indeterminate focal renal lesions qualitatively and concluded that CEUS is highly sensitive and specific in characterizing indeterminate renal masses [12]. The first study with quantitative CEUS in renal tumors from Aoki et al. described a shorter TTP for renal tumors compared renal parenchyma but no differences between different tumor entities [19]. Furthermore, they reported that malignant renal tumors enhance more quickly than surrounding renal parenchyma and have relative hyperenhancement at time to peak [19–21]. Xue et al. described that 88% of 84 renal cell carcinomas showed hyperenhancement in the cortical phase [4]. In a small cohort ($n = 12$), Kasoji et al. showed that PE provided significant differences between ccRCC, pRCC and chRCC [22]. It is described that oncocytomas may show some enhancement patterns similar to renal cell carcinomas [23]. We could show that oncocytoma and ccRCC differed from each other in PE, WI and TTP. Compared to previous studies reporting that oncocytoma is indistinguishable from ccRCC, we observed significant differences between ccRCC and oncocytoma. This inconstancy may be due to heterogeneity of lesions at different sizes or different grading may influence the enhancement patterns [22].

In our study, cystic lesions classified as category III showed no malignancy, but signs of chronic inflammation and fibrosis. Especially in case of infected cysts with mural enhancement there may be overlap between benign and malignant disease [23]. Recent studies reported a higher accuracy of CEUS compared to CT in the detection of wall and septa microvasculature in complex cysts [24, 25]. Thus, recent guidelines of the European Federation of Societies for Ultrasound in Medicine and Biology (EFSUMB) consider the characterization of complex cysts as one of the main indications for CEUS. The study from Barr et al. found a sensitivity of 100% and a specificity of 96.6%, with a positive predictive value of 91.5% and a negative predictive value of 100% in characterization of IRM [12]. With the introduction of quantitatively CEUS, it seems to be possible to differentiate different types of solid lesions.

Our study holds several limitations. First, it represents a single center experience. We only examined lesion < 4 cm, so larger tumors could show different behaviors due to hyalinization or necrosis at CEUS imaging. Examination time and imaging interpretation in ultrasound are dependent on the examiner, but quantification of CEUS imaging offers objectivity. A technical limitation is the lack of parallel ARFI and CEUS when using the fusion mode with CT, thus we used this step only to identify the lesion of interest. One major limitation of ARFI imaging itself is represented by the fact that elastography of pure cystic lesions and/or cystic lesions with septa does not provide useful information [26, 27]. Also, we did not obtain a histological diagnosis of benign cystic lesions but present a lengthy follow-up (minimum of 24 months).

In conclusion, characterization of small CT-indeterminate renal masses using acoustic radiation force impulse elastography and contrast-enhanced ultrasound as differentiation of ccRCC from oncocytoma and chRCC/pRCC seems possible and can support urological decision making.

Author contributions WMT: data collection, data analysis, manuscript writing and editing. JB: project development, data analysis, manuscript editing. SK: manuscript editing. DS: data analysis, manuscript editing. AS: project development, manuscript editing. KN: project development, manuscript editing. MH: data collection, manuscript editing. SK: project development, data collection, data analysis, manuscript writing and editing.

Compliance with ethical standards

Conflict of interest Konstantin Nikolaou is a member of the speakers' bureau of Siemens AG, Bracco Group and Bayer AG. All other authors declare no conflicts of interest.

Ethical approval All procedures performed in studies involving human participants were in accordance with the ethical standards of the institutional and/or national research committee and with the 1964 Helsinki declaration and its later amendments or comparable ethical standards.

Informed consent This prospective study was approved by the institutional review board (361/2015BO2), and informed consent was obtained.

References

1. Heilbrun ME, Remer EM, Casalino DD, Beland MD, Bishoff JT, Blaufox MD, Coursey CA, Goldfarb S, Harvin HJ, Nikolaidis P, Preminger GM, Raman SS, Sahni A, Vikram R, Weinfeld RM (2015) ACR appropriateness criteria indeterminate renal mass. J Am Coll Radiol JACR 12(4):333–341. https://doi.org/10.1016/j.jacr.2014.12.012
2. Kay FU, Pedrosa I (2017) Imaging of solid renal masses. Radiol Clin N Am 55(2):243–258. https://doi.org/10.1016/j.rcl.2016.10.003
3. Graumann O, Osther SS, Karstoft J, Horlyck A, Osther PJ (2015) Bosniak classification system: inter-observer and intra-observer agreement among experienced uroradiologists. Acta Radiol (Stockh Swed 1987) 56(3):374–383. https://doi.org/10.1177/0284185114529562
4. Xue LY, Lu Q, Huang BJ, Li Z, Li CX, Wen JX, Wang WP (2015) Papillary renal cell carcinoma and clear cell renal cell carcinoma: differentiation of distinct histological types with contrast-enhanced ultrasonography. Eur J Radiol 84(10):1849–1856. https://doi.org/10.1016/j.ejrad.2015.06.017
5. King KG, Gulati M, Malhi H, Hwang D, Gill IS, Cheng PM, Grant EG, Duddalwar VA (2015) Quantitative assessment of solid renal masses by contrast-enhanced ultrasound with time-intensity curves: how we do it. Abdom Imaging 40(7):2461–2471. https://doi.org/10.1007/s00261-015-0468-y
6. Silverman SG, Israel GM, Trinh QD (2015) Incompletely characterized incidental renal masses: emerging data support conservative management. Radiology 275(1):28–42. https://doi.org/10.1148/radiol.14141144
7. Gerst S, Hann LE, Li D, Gonen M, Tickoo S, Sohn MJ, Russo P (2011) Evaluation of renal masses with contrast-enhanced ultrasound: initial experience. AJR Am J Roentgenol 197(4):897–906. https://doi.org/10.2214/ajr.10.6330
8. Ng CS, Wood CG, Silverman PM, Tannir NM, Tamboli P, Sandler CM (2008) Renal cell carcinoma: diagnosis, staging, and surveillance. AJR Am J Roentgenol 191(4):1220–1232. https://doi.org/10.2214/ajr.07.3568
9. Prasad SR, Humphrey PA, Catena JR, Narra VR, Srigley JR, Cortez AD, Dalrymple NC, Chintapalli KN (2006) Common and uncommon histologic subtypes of renal cell carcinoma: imaging spectrum with pathologic correlation. Radiogr Rev Publ Radiol Soc N Am Inc 26(6):1795–1806. https://doi.org/10.1148/rg.266065010
10. Shuch B, Amin A, Armstrong AJ, Eble JN, Ficarra V, Lopez-Beltran A, Martignoni G, Rini BI, Kutikov A (2015) Understanding pathologic variants of renal cell carcinoma: distilling therapeutic opportunities from biologic complexity. Eur Urol 67(1):85–97. https://doi.org/10.1016/j.eururo.2014.04.029
11. Lu Q, Wen JX, Huang BJ, Xue LY, Wang WP (2015) Virtual touch quantification using acoustic radiation force impulse (ARFI) technology for the evaluation of focal solid renal lesions: preliminary findings. Clin Radiol 70(12):1376–1381. https://doi.org/10.1016/j.crad.2015.08.002
12. Barr RG, Peterson C, Hindi A (2014) Evaluation of indeterminate renal masses with contrast-enhanced US: a diagnostic performance study. Radiology 271(1):133–142. https://doi.org/10.1148/radiol.13130161
13. Finelli A, Ismaila N, Bro B, Durack J, Eggener S, Evans A, Gill I, Graham D, Huang W, Jewett MA, Latcha S, Lowrance W, Rosner M, Shayegan B, Thompson RH, Uzzo R, Russo P (2017) Management of small renal masses: American Society of Clinical Oncology Clinical Practice Guideline. J Clin Oncol 35(6):668–680. https://doi.org/10.1200/jco.2016.69.9645
14. Egbert ND, Caoili EM, Cohan RH, Davenport MS, Francis IR, Kunju LP, Ellis JH (2013) Differentiation of papillary renal cell carcinoma subtypes on CT and MRI. AJR Am J Roentgenol 201(2):347–355. https://doi.org/10.2214/ajr.12.9451
15. Nicolau C, Bunesch L, Pano B, Salvador R, Ribal MJ, Mallofre C, Sebastia C (2015) Prospective evaluation of CT indeterminate renal masses using US and contrast-enhanced ultrasound. Abdom Imaging 40(3):542–551. https://doi.org/10.1007/s00261-014-0237-3
16. Clevert DA, Stock K, Klein B, Slotta-Huspenina J, Prantl L, Heemann U, Reiser M (2009) Evaluation of acoustic radiation force impulse (ARFI) imaging and contrast-enhanced ultrasound in renal tumors of unknown etiology in comparison to histological findings. Clin Hemorheol Microcirc 43(1–2):95–107. https://doi.org/10.3233/ch-2009-1224
17. Goya C, Daggulli M, Hamidi C, Yavuz A, Hattapoglu S, Cetincakmak MG, Teke M (2015) The role of quantitative measurement by acoustic radiation force impulse imaging in differentiating benign renal lesions from malignant renal tumours. Radiol Med (Torino) 120(3):296–303. https://doi.org/10.1007/s11547-014-0443-7
18. Tamai H, Takiguchi Y, Oka M, Shingaki N, Enomoto S, Shiraki T, Furuta M, Inoue I, Iguchi M, Yanaoka K, Arii K, Shimizu Y, Nakata H, Shinka T, Sanke T, Ichinose M (2005) Contrast-enhanced ultrasonography in the diagnosis of solid renal tumors. J Ultrasound Med 24(12):1635–1640
19. Aoki S, Hattori R, Yamamoto T, Funahashi Y, Matsukawa Y, Gotoh M, Yamada Y, Honda N (2011) Contrast-enhanced ultrasound using a time-intensity curve for the diagnosis of renal cell carcinoma. BJU Int 108(3):349–354. https://doi.org/10.1111/j.1464-410X.2010.09799.x
20. Ignee A, Straub B, Brix D, Schuessler G, Ott M, Dietrich CF (2010) The value of contrast enhanced ultrasound (CEUS) in the characterisation of patients with renal masses. Clin Hemorheol Microcirc 46(4):275–290. https://doi.org/10.3233/ch-2010-1352
21. Siracusano S, Bertolotto M, Ciciliato S, Valentino M, Liguori G, Visalli F (2011) The current role of contrast-enhanced ultrasound (CEUS) imaging in the evaluation of renal pathology. World J Urol 29(5):633–638. https://doi.org/10.1007/s00345-011-0699-7
22. Kasoji SK, Chang EH, Mullin LB, Chong WK, Rathmell WK, Dayton PA (2017) A pilot clinical study in characterization of malignant renal-cell carcinoma subtype with contrast-enhanced ultrasound. Ultrasound Imaging 39(2):126–136. https://doi.org/10.1177/0161734616666383
23. Harvey CJ, Alsafi A, Kuzmich S, Ngo A, Papadopoulou I, Lakhani A, Berkowitz Y, Moser S, Sidhu PS, Cosgrove DO (2015) Role of US contrast agents in the assessment of indeterminate solid and cystic lesions in native and transplant kidneys. Radiogr Rev Publ Radiol Soc N Am Inc 35(5):1419–1430. https://doi.org/10.1148/rg.2015140222
24. Ascenti G, Mazziotti S, Zimbaro G, Settineri N, Magno C, Melloni D, Caruso R, Scribano E (2007) Complex cystic renal masses: characterization with contrast-enhanced US. Radiology 243(1):158–165. https://doi.org/10.1148/radiol.2431051924
25. Clevert DA, Minaifar N, Weckbach S, Jung EM, Stock K, Reiser M, Staehler M (2008) Multislice computed tomography versus contrast-enhanced ultrasound in evaluation of complex cystic

renal masses using the Bosniak classification system. Clin Hemorheol Microcirc 39(1–4):171–178
26. Dumitriu D, Dudea S, Botar-Jid C, Baciut M, Baciut G (2011) Real-time sonoelastography of major salivary gland tumors. AJR Am J Roentgenol 197(5):W924–W930. https://doi.org/10.2214/ajr.11.6529
27. Moon HJ, Sung JM, Kim EK, Yoon JH, Youk JH, Kwak JY (2012) Diagnostic performance of gray-scale US and elastography in solid thyroid nodules. Radiology 262(3):1002–1013. https://doi.org/10.1148/radiol.11110839

Affiliations

Wolfgang M. Thaiss[1] · Jens Bedke[2] · Stephan Kruck[2] · Daniel Spira[3] · Arnulf Stenzl[2] · Konstantin Nikolaou[1] · Marius Horger[1] · Sascha Kaufmann[1]

Wolfgang M. Thaiss
wolfgang.thaiss@med.uni-tuebingen.de

Stephan Kruck
stephan.kruck@med.uni-tuebingen.de

Daniel Spira
daniel.spira@med.uni-heidelberg.de

Arnulf Stenzl
arnulf.stenzl@med.uni-tuebingen.de

Konstantin Nikolaou
konstantin.nikolaou@med.uni-tuebingen.de

Marius Horger
marius.horger@med.uni-tuebingen.de

Sascha Kaufmann
sascha.kaufmann@med.uni-tuebingen.de

1 Department of Diagnostic and Interventional Radiology, Eberhard-Karls-University Tübingen, Hoppe-Seyler-Strasse 3, 72076 Tübingen, Germany

2 Department of Urology, Eberhard-Karls-University Tübingen, Hoppe-Seyler-Strasse 3, 72076 Tübingen, Germany

3 Diagnostic and Interventional Radiology, University Medical Center Heidelberg, Im Neuenheimer Feld 110, 69120 Heidelberg, Germany